One-pot facile biosynthesis of copper nanoparticles using Dillenia indica L. bark extract for in vitro anticancer activity against human lung and breast cancer cell lines

Larica Mohanta
CSIR- Institute of Minerals and Materials Technology
Bhabani Sankar Jena (bsjena@immt.res.in)
CSIR- Institute of Minerals and Materials Technology

Research Article

Keywords: Dillenia indica, Green Synthesis, Phytochemicals, Copper Nanoparticles, Anticancer

Posted Date: November 29th, 2022

DOI: https://doi.org/10.21203/rs.3.rs-2311167/v1

Abstract

The current study focused on green synthesis of copper nanoparticles (CuNPs) using ethanolic bark extract of *Dillenia indica* L. as an eco-friendly, non-toxic reducing agent as well as surface stabilizing agent. The phytochemical screening showed higher positivity of phenolics and flavonoid compounds in the bark extract. Biosynthesized CuNPs was optimized and characterized using UV-Visible spectrophotometer, Transmission electron microscope (TEM), Particle size analyser, and Fourier Transform Infrared Spectroscopy (FTIR). UV-Visible spectroscopic analysis showed maximum wavelength at 512 nm indicating the formation of CuNPs. TEM analysis reveals spherical shaped, well dispersed CuNPs with size ranging from 5 to 30 nm. Obtained CuNPs were stable up to one month with zeta potential value of -41.8 mV. FTIR analysis of CuNPs showed that the phytoconstituents of *D. indica* L. bark extract were the contributing factors for the reduction of copper ions as well as capping and surface functionalization of CuNPs for their stability in aqueous medium. Further, the bio-synthesized CuNPs showed dose and time dependent cytotoxicity against human lung cancer (A549) and breast cancer (MCF-7) cell lines. Morphological alterations due to apoptosis was studied by acridine orange/ethidium bromide and DAPI stains through fluorescence microscopy which reveals cell shrinkage, nuclear fragmentation, and blebbing in CuNPs treated cancer cells. Therefore, the present study unveiled the cytotoxic efficacy of *D. indica* mediated CuNPs induced apoptosis in A549 and MCF-7 cells which could be further used as a contemporary strategy for cancer therapy.

1 Introduction

In recent years' nanotechnology circumscribed an increasing impact on industrial and medical research accounting to find solutions across a wide range of physicochemical and biomedical science. Development of different inorganic and organic nanomaterials exhibit completely different properties, as they have distinct features including distribution, size, and shape which act as crossroads of multiple applications in biotechnology including tissue engineering, drug delivery, imaging, diagnostics, electronics, textile and food packaging industries [1].

The scientific community has customized many suitable synthesis techniques for the production of nanoparticles according to their applications. However, various physico-chemical approaches for the synthesis of metal nanoparticles have their disadvantages such as the use of hazardous chemicals as reducing agents, expensive, and time-consuming process [2]. Green nanotechnology has become a new trend in nanoparticle production due to its several advantages such as eco-friendly, reproducibility in production, easy scaling-up and less expensive [3]. In this regard, several biological reducing agents such as plants (extracts of the whole plant, plant parts & plant derived phytochemicals), microorganisms (bacteria, fungi, yeast, algae) and biomolecules (proteins, carbohydrates, and nucleic acids) are used for nanomaterial synthesis. Among these, plant-mediated nanoparticle production has been regarded as an economical, stable, and environmentally friendly technology [4, 5].

Among various metal nanoparticles, copper nanoparticles have received a lot of attention in the domains of nanotechnology and nanomedicine over last ten years, because of being more economical to be utilized efficiently in catalytic, sensors, optical, electrical, agricultural and biomedical applications [6]. Copper is an effective trace element involved in the nutrition system of living organism [7]. The unique properties of CuNPs such as high surface to volume ratio, ductility, strength and yield makes it a potentially cost-efficient nanomaterial to be used in various therapeutic applications such as catalytic, antioxidant, antimicrobial, antifungal and cytotoxic activities [8]. The thermal reduction, laser ablation, microemulsion, polyol method, etc. have been used for production of CuNPs [9]. However, due to ease-of-use and environmental compatibility, the biological production of CuNPs employing plants as bioreducers has been studied to overcome the restrictions occurred due to physical and chemical methods.

Dillenia indica L. belongs to family Dilleniaceae is a medicinal plant found in sub-himalayan region of tropical Asian continent. As reported, extracts from plant parts have extraordinary properties like antidiabetic [10], antioxidant [11], anti-microbial, anticancer properties [12] etc. It contains host of secondary metabolites like lupeol, betulinaldehyde, betulinic acid, myricetin, sitosterol and stigmasterol [12] which helps in synthesizing biocompatible CuNPs with greater stability. Mohanty and Jena [13] reported the synthesis of AgNPs using *D. indica* bark extract which exhibits increased antioxidant and catalytic activities.

The thirst of searching most effective and appropriate drugs for treatment of cancer has been evolved as a challenging task in recent years because of increasing number of cancer deaths. The use of chemotherapy, radiation therapy, cancer related drugs for treatment of cancer also affects normal cells leading to neuron damage and skin problems [14]. Hence, there is an urgent requirement for development of potent, cost-effective cancer treatment method for the benefit of mankind.

In the last ten years lung cancer have emerged as a dreadful disease-causing millions of deaths worldwide. It was evaluated that near about 1.6 million deaths has occurred through lung cancer worldwide in 2012 [15]. Similarly, breast cancer is most common in case of females which accounts for 1 in 3 of each new females every year. Lung's cancer is the leading cause of death in men and second highest in women (after breast cancer) [16]. The main cause of lung cancer is attributed to increased intake of tobacco and smoking which causes nearly 30% of all deaths [17]. Excessive consumption of alcohol also leads to different types of cancer such as mouth, liver, breast, stomach, ovaries, etc. Other environmental factors causing cancer are absorption of UV-radiation, occupational exposure to organic and inorganic substances, infectious microorganism, obesity, hormonal therapy (breast cancer), air and water pollution [18]. The rise of cancer over time has challenged the researchers to find out new, favourable and environment friendly cancer remedies.

Singh et al. [19] studied the *in vitro* anticancer activity of green synthesized AgNPs using leaf extract of *Carissa carandus* against hepatic (HUH-7) and renal (HEK-7) cell lines. Synthesis of AgNPs using endophytic fungi *Botryosphaeria rhodina* exerts cytotoxic properties on A549 cell lines through radical scavenging and apoptosis [20]. The findings suggested that the active biomolecules present in the fungi

may be responsible for the cytotoxic activity of AgNPs in *in vitro* conditions. Similarly, concentration dependent cytotoxicity of enterococcus-mediated AuNPs against human colorectal cancer cells (HT-29) was observed by Vairavel et al. [21]. Morphological changes occurring due to apoptosis was also observed. Shwetha et al. [22] prepared ZnONPs using *Areca catechu* extract as reducing agent attributes potential cytotoxicity against MCF-7 cell line.

A study by Valodkar et al.[23] on biosynthesized copper nanoparticles using medicinal plant *Euphorbia nivulia* L. has indicated biological consequences on tumour cells. *In vitro* anti-cancer activity of *Eclipta prostata* leaf extract mediated synthesis of CuNPs was demonstrated by Chung et al.[24] against HepG2 cell lines. CuONPs also exhibited anticancer potency against HeLa cell lines in concentration dependent manner [25]. Manikandan et al.[26] bio fabricated CuONPs using leaf extract of *Ocimum americanum* which showed potent cytotoxic activity in A549 cancer cell lines. Hasanin et al.[27] observed the cytotoxic activity of CuNPs-starch nanocomposites against breast cancer cell lines.

In this background, the present research was focused on biosynthesis of CuNPs using ethanolic bark extract of *Dillenia indica* as reducing as well as stabilizing agent. The cytotoxic ability of biosynthesized CuNPs was studied against human lung cancer (A549) and breast cancer (MCF-7) cell lines. The current report provides comprehensive details regarding biosynthesis and anticancer activities of CuNPs which will have a remarkable impact on biomedical applications.

2 Materials And Methods

2.1 Chemicals

Copper chloride ($CuCl_2$. $2H_2O$) (Analytical grade) was procured from Himedia, Mumbai. All chemicals and solvents were purchased from Merck in Mumbai, India. 3-(4, 5-Dimethylthiazol-2-yl-)- 2,5-diphenyltetrazolium bromide (MTT), DAPI, Dulbecco's Modified Eagle Media (DMEM) and fetal bovine serum (FBS) were purchased from Himedia, Mumbai.

2.2 Preparation and Extraction of *D. indica* bark extract

Extraction and preparation of *D. indica* bark extract was done according to Mohanty and Jena [13] with some minor modifications. The trunk barks were collected from an age-old *D. indica* plant in CSIR-IMMT Campus, Bhubaneswar, Odisha, India followed by proper washing to remove dirt. These were allowed to dry for 4 days and grounded to fine powder (mesh size 60). Extraction of nonpolar compounds was done by dissolving 100 g of bark powder in 1L of hexane for 6 h. Further the dried powder was dissolved in 80% ethyl alcohol in order to extract highest amount of polyphenols. The extraction was repeated twice followed by filtration using Whatman No. 41 filter paper. The required bark extract was obtained by concentrating the solvent in a rotary vacuum evaporator at 45°C and was stored at 4°C for further use.

2.3 Phytochemical Screening Test

The qualitative screening analysis was done to establish the presence of several active phytoconstituents such as phenols, flavonoids, alkaloids, steroids, terpenoids in the ethanolic bark extract of *D. indica*. The analysis was done according to the standard protocols reported [28, 29] [30]

2.4 Synthesis and optimization of CuNPs using ethanolic bark extract of *D. indica*

Copper nanoparticles were synthesized by adding bark extract (2mg/mL) dissolved in aqueous medium to $CuCl_2$. $2H_2O$ solution (1mM) following adjustment of pH to 10 by adding 10 mM NaOH. The reaction mixture was heated to 60°C in a hot water bath for 15 minutes. The formation of CuNPs was confirmed by the appearance of wine-red colouration. The coloured mixture was centrifuged at 12000 rpm for 20 mins and obtained pellet was washed thrice with distilled water to remove any unbound biological molecules followed by drying at hot air oven to obtain fine powder which was used for further analysis. However, the synthesis of CuNPs were optimized by considering the effect of different reaction parameters such as concentration of copper salt (0.1, 1, 10 mM), concentration of bark extract (1, 2, 4 mg/mL), temperature (50, 60, 80, 90°C) and pH (4, 7, 10, 11, 12) of the medium.

2.5 Characterization of CuNPs

The synthesis of CuNPs was monitored between 300 to 800 nm and measured in UV–Visible spectrophotometer (Eppendrof Biospectrometer). Synthesized nanoparticle solution was stored at ambient temperature. The stability of CuNPs was monitored by UV spectral analysis for up to one month. The structural morphology and size of the nanoparticles were obtained from a TEM (FEB Tecnai G2 20, Netherlands) analyser. The CuNPs solution was sonicated for 10 mins at 40 hz prior to analysis using ultrasonic homogenizer for proper dispersion (Model 3000 MP, Biologics, Virginia, USA). On the carbon-coated copper grid, a drop of the CuNPs solution was poured, and dried under a lamp for one hour. Particle size distribution and Zeta potential of synthesized CuNPs were analyzed using a Dynamic light scattering unit (Anton Paar Litesizer 500). Sample was prepared with 20µl of synthesized CuNPs in 1mL of deionised water. The FT-IR spectra of the *D. indica* bark extract and CuNPs were obtained by using Bruker Alfa II spectrophotometer in the transmittance range between 4000 to 500 cm^{-1} to identify the surface functional groups which are capable of reduction and formation of CuNPs.

2.6 Cytotoxic Activity of CuNPs: *In vitro*

2.6.1 Cell Culture

A549 (Adenocarcinoma human alveolar basal epithelial) and MCF-7 (breast cancer) cell lines were obtained from Imgenex, Bhubaneswar, India. The cells were kept in an incubator at 37°C with a supply of 5% CO_2 and were nourished with DMEM containing 10% FBS and 1% antibiotic-antimycotic solution. For all experiments, cells were seeded to produce an experimental stage of 80% confluency in cell culture flasks or well plates. The flasks/plates were observed under a phase contrast inverted microscope (Leica DM IL LED) to detect morphological changes and photographed using a camera.

2.6.2 Cell Viability Assay

Effect of synthesized copper NPs, copper chloride and extract on cell proliferation was evaluated using MTT assay. The tests were conducted on white corning 96-well plates (Corning, Costar, NY). In the current investigation, cells were seeded in a 96-well plate at a density of 1×10^5 cells per well prior to the experiment and maintained in a CO_2 incubator at 37^0C and 5% CO_2 for 24 hours. Following 24 h growth, the medium was changed with fresh media and the cells were treated with eight different concentrations of synthesized NPs (30–240 µg/mL) for 24 and 48 hours. Well containing cells without any treatment were used as negative control and metal salt solution (1mM) and *D. indica* bark extract (2mg/mL) as used for synthesis of CuNPs were included as positive controls. After 24 and 48 hours, 20 µl of MTT solution (5 mg/mL) was added to each well. Then the plates were allowed for an additional 4 hours for reduction of MTT to formazan. After incubation period, media was discarded and washed with PBS. To dissolve the formazan crystal, 100 µl of MTT solubilisation solution (DMSO) was administered to each well. The absorbance of 96 well plates was measured at 490 nm by using a micro plate reader (iMARK TM Micro Plate Reader, Bio-Rad Laboratories Inc. USA). The percentage of the control was used to express values (incubated with media alone). Each cell line underwent two separate experiments with triplicates of each condition. The following formula was used to calculate the percentage of cell viability:

$$\% \text{ of Cell viability} = \frac{(\text{Abs of Control} - \text{Abs of Sample})}{\text{Abs of Control}} \times 100$$

2.6.3 Morphology Study

The A549 and MCF-7 cells cultured in 6 well plates were exposed to higher concentration of CuNPs (240 µg/mL) in order to obtain clear image of morphologically varied cells after achievement of 80% confluency with a monolayer. After 24 hours, media was removed and cells were washed with sterile PBS. Then morphology of control and treated cells were observed under phase contrast microscope. For this study, cells without any treatment were used as negative control and cells treated CuNPs were included as positive controls.

2.6.4 Dual Fluorescent Dye (AO/EtBr) Staining

Nuclear staining using acridine orange/ethidium bromide (AO/EtBr) dual fluorescent stain, was used to analyze the apoptosis in A549 and MCF-7 cell lines (1×10^5). The cells were treated separately with CuNPs (240 µg/mL), $CuCl_2$ (1mM) and extract (2mg/mL) solution separately in 6 well plates and incubated for 24 hours. After overnight incubation, the cells were given a mixture containing 20 µl of AO/EtBr staining solution in 1:1 ratio (100µg/mL in PBS). After 5 min, the cells were visualized under fluorescence microscope (Leica, DM3000). Based on the emission of green, orange, and red florescence for live, apoptotic, and necrotic cells, respectively, the treated cells were separated from one another.

2.6.5 Assessment of Nuclear Damage by DAPI Staining

In this study, the cyto-morphological changes in the nuclei of control and treated MCF-7 and A549 cells were assessed using the DAPI (4', 6-diamidino-2-phenylindole) stain. This staining method was done according to [31] with slight modifications. Cells were treated with CuNPs (240 µg/mL), $CuCl_2$ (1mM) and extract (2mg/mL) for 24 h and 48 h in a humidified atmosphere of 5% CO_2 at 37ºC. After incubation cells were gently scraped and harvested by centrifugation. The cells were fixed for 10 minutes at room temperature with 4% paraformaldehyde, and then mounted with DAPI (2.5 g/mL). The morphological changes were observed using fluorescence microscopy (Leica, DM3000).

2.7 Statistical Analysis

All the data were statistically analysed by ANOVA using Tukey's test in GraphPad Prism 8 software. Values depicting $p < 0.05$ were considered statistically significant between the treated and control groups. Experiments on cell viability were carried out in triplicate and the results were expressed as mean ± standard error of mean (SEM).

3 Results And Discussion

3.1 Phytochemical Screening Analysis

Plant extract acts as an efficient substitute for reducing and capping agents due to the presence of various bioactive compounds like phenols, flavonoids, terpenoids, steroids, glycosides, tannins, etc. The present phytochemical screening of ethyl alcoholic extract of *D. indica* indicated the presence of phenolics and flavonoids as the major constituents in addition to saponins, alkaloids, steroids, and tannins which corroborates with the results obtained by Deepa and Jena [11] (Table.1). Reports on different plants also specified the presence of the above compounds involved in reduction and stabilization of metal and oxides nanoparticles. Weng et al. [32] observed the presence of flavonoids, alkaloids and chlorophyll in the leaf extract of *Eucalyptus* which work as a reducing and capping agent for synthesis of Fe and AgNPs.

Table 1
Qualitative screening analysis of *D. indica* bark extract

Sl. No	Secondary metabolites	Test	Observation	Results
1	Phenols	Ferric chloride test	Bluish black or Violet	++
2	Flavonoids	Alkaline reagent test	Intense yellow or orange	++
3	Alkaloids	Mayer's test	Yellow	+
4	Tannins	Lead acetate test	White turbid	+
5	Saponins	Froth test	Appearance of foam	-
6	Terpenoids	Salkowski test	Reddish brown	-
7	Steroids	Salkowski test	Red colour in upper layer	+

*Here (++) represents high intensity of phytoconstituents, (+) presence and (-) absence of phytoconstituents

3.2 Role of Phytoconstituents in Reduction and Stabilization of CuNPs

Plant phytoconstituents play a major role in the reduction and capping of metal's nuclei for production of nanoparticles. The bark of *D. indica* L. contains phytochemicals like betulinaldehyde, betulinic acid, betulin, lupeol, myricetin and dillenetin [12]. As mentioned, the qualitative screening showed the presence of various secondary metabolites such as phenols, tannins, alkaloids, flavonoids, saponins with phenols and flavonoids as highest concentration. The functional groups of these phytochemicals are carboxylic, alkanes, aromatic rings, hydroxyl, and carbonyl having key role in the reduction of copper ion to formation of copper nanoparticles of controlled shape and size.

For possible mechanism in the synthesis CuNPs in this present study, we propose the role of myricetin one among the various biomolecules present in *D. indica*. It is hypothesized that the reactive hydrogen atom from myricetin is released during tautomeric transformation reaction of the enol form to keto form which helps in reduction of copper ions to generate CuNPs (Fig. 1). The divalent or monovalent valence states of copper metal ion is transformed to zero- valence state copper nuclei during the synthesis process. Further these nuclei combine to form CuNPs of various forms in nucleation process [33].

3.3 Biosynthesis of CuNPs

Biogenic synthesis of nanoparticles using plant as reducing agents gains advantages over other biomaterials because of being cost effective, easy availability, safe handle, easy scale up, etc. In this context, a single step process was achieved for synthesis of CuNPs using ethanolic bark extract of *Dillenia indica* which reduces Cu^{2+} ion of copper chloride solution to Cu^{0}. The main factor used to support the synthesis of CuNPs was the colour change of the reaction mixture, which was observed using UV-visible spectroscopy. Addition of bark extract to $CuCl_2$ solution changes the colour of the reaction mixture

from light yellowish to wine red indicating the formation of CuNPs (Fig. 2). Changing of the colour of reaction mixture is attributed to surface plasmon resonance (SPR) phenomenon.

3.4 Optimization of Reaction Parameters on Synthesis of CuNPs

The synthesis procedure of copper nanoparticles was optimized by taking consideration of variables like concentrations of *D. indica* bark extract (1, 2, 4 mg/mL), concentration of metal salt solution (0.1, 1, 10 mM), mixing ratio of bark extract and salt solution, pH (4, 7, 10, 11, 12) and temperature (40, 50, 60, 80, 90°C).

The amount of bark extract used performs a significant role in the transformation of metal ions into nanoparticles. The mixing ratio of bark extract with $CuCl_2$ solution in the synthesis process has been measured by UV- visible spectrophotometer (Fig. 3a). The data revealed that the strength of the SPR peak increases with the amount of bark extract as it approaches the optimal level at a ratio of 1:4. (Extract: $CuCl_2$). The reactions were conducted at pH 10. Similarly, increasing the concentration of bark extract from 2 mg/mL to 4 mg/mL increases the formation of CuNPs but the NPs formed were of larger size as visualized through TEM (Fig. 3b). However, further increasing the concentration leads to agglomeration of CuNPs which may be due to presence of excessive biomolecules present in the extract initiating secondary reaction on the surface of nuclei, thus increasing the particle size [34]. Therefore, the optimal concentration of bark extract was 2 mg/mL for synthesis of CuNPs.

The effect of precursor salt concentration on the formation of CuNPs was studied between 0.1, 1 and 10 mM $CuCl_2$ solution (Fig. 3c). Optimization of initial concentration of metal salt is required in order to obtain smaller sized NPs with desired shape. The present analysis showed that an increase in the concentration of $CuCl_2$ from 0.1 to 1 mM leads to formation of smaller sized CuNPs without agglomeration but further increasing the concentration yields large sized and agglomerated CuNPs. A similar outcome was reported using *Azadiracta indica* leaf extract for the reduction of copper ions [34]. Therefore, the optimum precursor salt concentration for synthesis of CuNPs was 1mM.

Another important parameter for synthesis of metal NPs is the pH of the reaction mixture. Variation in pH affects morphology and stability of the NPs. In the present study of nanoparticle synthesis, simply mixing of bark extract to $CuCl_2$ solution didn't lead to the formation of CuNPs. However, after altering the pH of the medium from acidic to alkaline by adding 10mM NaOH, CuNPs were obtained (Fig. 3d). These findings were further supported by [35] who synthesized CuNPs using leaf extract of *Dodonaea viscosa* for obtaining spherical shaped copper nanoparticles at pH 10. The importance of pH for synthesis of CuNPs was also reported [36]. At pH 4 no absorbance peak was observed and the colour of the solution was yellow. Increasing the pH to 10 and 11 colour changes to deep red and absorbance peak was observed at 512 nm and 510 nm. At pH 12 the absorbance peak broadens and agglomeration of CuNPs was observed due to presence of impurities and unbound particles such as Cu_2O, Cu $(OH)_2$. Therefore, in the present study optimum pH for synthesis of CuNPs was established at pH 10.

The effect of temperature also plays an important role influencing the synthesis process of CuNPs. It was observed that the rate of conversion of Cu^{2+} ions to Cu^{0} increased considerably by varying temperature range from 40 to 90°C, but the synthesis rate increased up to 60°C (Fig. 3e). At higher temperature, agglomeration and large sized CuNPs were formed containing impurities as observed in TEM analysis. Therefore, the optimum temperature of the reaction medium for synthesis of CuNPs was established at 60°C. Reports showed optimization and synthesis of CuNPs at 60°C using *Dodonaea viscosa* extract as bioreductant [35].

Therefore, the reaction mixture containing 2mg/mL of *D. indica* bark extract dissolved in aqueous medium was added to 1mM $CuCl_2$. $2H_2O$ at pH 10 and kept in a hot water bath for 15 mins at 60°C was considered to be the optimum synthesis conditions for copper nanoparticles as monitored by UV-visible spectrophotometer.

3.5 Characterization of Synthesized CuNPs

In the present study, we report a cost-effective, eco-friendly and easy procedure for the synthesis of the CuNPs using ethanolic bark extract of *Dillenia indica* L. as a reducing and capping agent. The biosynthesis of CuNPs was preliminarily confirmed by UV-visible spectrophotometer. The CuNPs obtained was characterized by Particle Size Analyser, TEM and FTIR and were found to be stable for one month.

3.5.1 UV-Visible Spectroscopic Analysis

A UV-visible spectrophotometer was used to examine the synthesis of copper nanoparticles obtained by reducing metal ions using *D. indica* bark extract as bioreducer. The formation of CuNPs was indicated by the appearance dark wine-red colour with maximum wavelength of 512 nm due to vibrations in surface plasmon resonance and reduction of copper chloride ions by *D. indica* bark extract (Fig. 4a). A per reports, the absorption bands for CuNPs were found in the range of 500–600 nm [37]. The absorbance peak of *D. indica* bark extract was observed at 440 nm. Production of CuNPs occurs due to the presence of active biomolecules from bark extracts which were mostly accountable for reduction of Cu^{2+} ions. The synthesized CuNPs were found to be stable for up to one month with no change in the position and symmetry of the absorption peak which depicts capping of phytoconstituents of *D. indica* extract on the surface of NPs thereby protecting it from agglomeration and decomposition (Fig. 4b). CuNPs synthesized using *Euphorbia prolifera* leaf extract were also quite stable up to one month with no significant difference in the position of absorption peak [38].

3.5.2 Particle Size Analyzer

The particle size distribution of synthesized CuNPs was measured using Dynamic Light Scattering (DLS) unit. The particles formed were monodisperse with average particle size of 54 nm (Fig. 5a). CuNPs' polydispersity index (PDI) was found to be 0.33 which showed that the NPs were evenly scattered in water. The amount of electrostatic repulsion between neighbouring and similarly charged particles in the dispersion is indicated by the value of zeta potential. Higher stability of NPs is indicated by the large

magnitude of the zeta potential value [34]. The average zeta potential value of synthesized CuNPs has been found at -41.8 mV (Fig. 5b) suggesting highly stable CuNPs. The -ve zeta potential value was may be due to the phenolics compounds present in the bark extract acting as capping agent for NPs which also contributed for their stability as seen in UV-visible spectrophotometric study for one month. We have also obtained high level of positivity of phenolics in the extract during phytochemical screening (Table-1). Moreover monodisperse copper nanoparticle provides a useful attribute for material scientists to improve biomedical applications associated with copper nanoparticles.

3.5.3 TEM Analysis

Transmission electron microscope provided further insight into the morphology and size of the CuNPs. The TEM micrograph (Fig. 6) revealed well dispersed, spherical CuNPs with size ranging from 5 to 30 nm. Similar results were also observed from TEM micrographs of copper nanoparticles synthesized using *Dodonaea viscosa* leaf extract with size ranging between 30–40 nm exhibiting spherical shape [35]. According to Chung et al. [24] copper nanoparticles were biosynthesized using *Eclipta prostrata* leaf extract, and TEM investigation showed that the NPs were spherical in form with size varying from 28 to 45 nm.

3.5.4 FTIR Analysis

The FTIR spectroscopic analysis was carried out to identify the possible biomolecules present in the crude bark extract responsible for capping and reducing copper metal ions into CuNPs. Figure 7 spectra showed the presence of different peaks of biosynthesized CuNPs and *D. indica* bark extract at a different wavelength related to the nature of functional groups. Table 2 demonstrates the functional groups of the phytochemicals present in the *D. indica* bark extract which might help in the capping and stabilization of CuNPs. A prominent peak found at 1641 cm^{-1} in the *D. indica* bark extract might occur due to the C = C stretching vibration of the aromatic phenols, which was displaced to 1634 cm^{-1} in case of CuNPs suggesting the phenolic compounds interaction with the nanoparticles [35]. Another band at 2368 cm^{-1} in extract indicated the C-H stretching vibrations of $-CH_3$ groups found in terpenoids and in case of nanoparticle it was shifted to 2128 cm^{-1}. Peak at 1357 cm^{-1} attributed to -C-N stretch of aromatic amine [38]. The presence of peak at 3321 cm^{-1} and 3327 cm^{-1} could be due to intermolecular and intramolecular interactions of O-H group in polyphenols or proteins or polysaccharides. Protein-metal nanoparticles interaction occurs through the unbound amine groups or carboxylate ion of amino acid residues [39]. The peak observed at 1004 cm^{-1} attributed to the stretching vibration of C and O bond among alcohol and carboxylic groups [40]. The decreased transmittance observed at 516 cm-1 in bark extract was shifted to 523 cm-1 which indicates association of aromatic biomolecules found in the bark extract in the reduction of Cu2 + ions. The observation of a common band in the bark extract of *D. indica* and CuNPs suggests the presence of bioactive compounds like terpenoids, phenolics, flavonoids and glycosides on the surface of synthesized CuNPs [12].

Table 2
Functional groups present on the surface of biosynthesized CuNPs in comparison to that present in bark extract

Functional Group	*D. indica* bark extract (cm^{-1})	CuNPs (cm^{-1})
O-H	3321	3327
-C-H-	-	2818
-C-H-	2368	2128
-C = C-	1641	1634
-C-N-	-	1357
-C-O	1085	1004
-C = C-	889	-
-C = C-	618	618
Halogen compound	516	523

3.6 Anticancer Activity *in vitro*

In the present study the anticancer potentials of green synthesized copper nanoparticles were evaluated against human lung cancer cells (A549) and human breast cancer cells (MCF-7) through MTT assay for cell viability, cellular morphology and apoptotic cell death through nuclear staining using AO/EtBr and DAPI dyes.

3.6.1 Cell Viability Assay

The MTT colorimetric test was used to determine cell viability. It is based on the ability of mitochondrial NAD (P) H-dependent oxidoreductase enzyme to convert yellow tetrazolium (MTT) dye into insoluble formazan crystal which has purple colour. The insoluble formazan can be dissolved in DMSO. The rate of formazan crystal formation is directly correlated to cell viability which is measured in terms of optical density at 490 nm using a micro plate reader. To assess the cell viability of A549 and MCF-7 cell lines, the cells were treated with CuNPs at different concentrations (0, 30, 60, 90, 120, 150, 180, 210, 240 µg/mL) for time interval of 24 and 48 h followed by MTT assay. It was observed that inhibition of cell growth on nanoparticles manifested A549 and MCF-7 cell line occurs in dose-dependent as well as time-dependent manner which corroborates with the study done by Sankar et al. [41]. The synthesized CuNPs was more effectively inhibiting cell growth as compared to *D. indica* bark extract and the metal salt solution (Fig. 8b & d). The biosynthesized CuNPs at lower concentration against A549 cell lines (30 µg/mL) showed 81 % nd 71% viability in 24 and 48 h whereas at higher concentration (240 µg/mL) the cell viability decreased up to 17 % nd 8% in 24 and 48 h of incubation period respectively (Fig. 8a). Similarly, the dose- dependent toxicity of CuNPs against MCF-7 cell lines also revealed decreased cell viability up to 26 % nd 17 % t

higher concentration (240 µg/mL) after 24 h and 48 h of incubation period respectively (Fig. 8c). The half maximal inhibitory concentration (IC_{50}) of synthesized CuNPs solution against A549 and MCF-7 cell lines were observed to be at 120 µg/mL. The figure depicts significantly differing outcomes ($p < 0.05$) between control and treated groups of A549 and MCF-7 cell lines respectively. The increased cellular toxicity of biosynthesized CuNPs on both the cell lines in comparison to extract and metal ion solution may be due to the increased surface area of nanoparticles and surface functionalization of nanoparticles with bioactive compounds of *D. indica* bark extract which plays as an encapsulating agent in copper nanoparticles. The cytotoxicity of biosynthesized CuNPs in A549 cell lines was also reported by [42]. Hasanin et al. [27] reported the anticancer efficiency of myco-synthesized CuNPs with IC_{50} at 210 µg/mL. Concentration and dose dependent decrease in cell viability was also observed in MCF-7 cell lines treated with CuONPs [43]. Moreover, increasing the concentration of CuNPs and period of incubation time from 24 h to 48 h leads to decrease in the number of viable cells which demonstrates the efficiency of the biosynthesized CuNPs in a dose and time dependent manner.

3.6.2 Effect on Cell Morphology

In order to validate the outcomes of cell viability experiment we further studied the effect of synthesized CuNPs induced morphological alterations in A549 and MCF-7 cell lines for 24 h and 48 h of incubation.

Under a phase contrast inverted microscope, the morphological changes of CuNPs-treated A549 cells were studied. This indicated clumped, wrinkled forms and an increased number of dead cells (Fig. 9). The control A549 cells exhibited normal morphology with long fusiform shape, tiny size, distinct cell borders and highly adherent-pebble like development which corroborated with the results of [44]. Literature survey did not show study of the morphological variations in CuNPs treated A549 cells. However, [28] observed the morphological changes in the A549 cell lines treated CuONPs synthesized using different leaf extracts which exhibited cell shrinkage, nuclear fragmentation and cytoplasmic vacuolation.

As shown in image the control MCF-7 cells were polygonal in shape whereas after treatment with CuNPs the shape changes to round or narrow leading to growth retardation and inferior adherence (Fig. 9) under phase contrast inverted microscope. Solairaj et al. [45] studied the anticancer activity and cellular morphology of CuNPs against MCF-7 cells which showed that control cells retained their polygonal shape whereas CuNPs treated cell showed distinct structural alterations like shrinkage and blebbing.

3.6.3 Nuclear Staining

To further support the cytotoxic activities of CuNPs, nuclear staining using dual staining method was carried out to check the plausible mechanistic cell death. Following the evaluation of cell morphology, the induction of apoptosis by nanoparticles in A549 and MCF-7 cells was verified by the differential uptake of fluorescent DNA-binding dyes, such as acridine orange/ethidium bromide staining (AO/EtBr). Here we have used AO/EtBr dual staining method to distinguish the live and dead cells. While EtBr is a membrane impermeable dye that only stains the DNA of membrane compromised/dead cells, AO is a membrane permeable dye that stains both viable and injured cells. As a result, cells stained with AO appears green

because their membranes are intact, while cells stained with EtBr (cells devoid of cytoplasm) appear orange or red because of nuclear shrinkage or blebbing. Cells stained with dual dyes have green cytoplasm and yellow-orange nuclei.

Cells were grown in a 96-well plate, and the treatment was carried out as previously indicated. The cells treated with CuNPs (240 µg/mL) were found to be greenish yellow at early stage whereas at later stage the apoptotic cells become more concentrated and asymmetrical showing reddish orange in colour due to cell death (Fig. 10a & b). Sankar et al. [41] treated A549 cells with CuONPs and observed apoptosis induction and orange shattered nuclei compared to control cells. The control cells without any treatment appear to be green due to intact mitochondrial membrane. The cells treated with extract and metal salt solution as positive control appears as mixture of both live and dead cells. This result correlates with MTT assay results, where we found that there is decrease in number of viable cells in case of extract and $CuCl_2$ solution. Morever, the number of membranes blebbed rounded cells increases with increase in incubation time. The degree of apoptotic death of A549 and MCF-7 treated cell line was in the order of CuNPs > Metal salt > extract.

3.6.4 DAPI Staining

One of the mechanisms used to inhibit cell development is apoptotic cell death. DAPI is a nuclear-specific blue fluorescent dye with a stronger affinity for DNA's A/T-rich sections. This fluorescent tag was used to quantify the proportion of apoptotic cells with condensed and fragmented chromatin as well as to highlight the nuclear alterations that occur during apoptosis [46, 47]. From the 24 h to 48 h of CuNPs treatment, the nuclear morphological analyses revealed a rise in the number of cells with small, condensed nuclei, indicating a growing number of apoptotic cells with increasing period of incubation (Fig. 11a & b). Apart from nuclear condensation the stained cells appeared to lose their structure with the increasing incubation period from 24 to 48 h. The numbers of apoptotic cells were significantly higher in CuNPs treated groups as compared to control cells. The control cells tend to maintain their shape and size. Thus, this staining revealed the morphological changes in CuNPs treated cells in terms of both DNA disintegration and chromatin condensation. Baharara et al. [48] observed the DNA fragmentation in MCF-7 cells treated with biosynthesized AgNPs using DAPI fluorescent stain.

3.6.5 Hypothetical Mechanistic Insight to Cytotoxicity

Absorption of metal nanoparticles into the systemic circulation of human body mainly depends upon their physicochemical properties which contributes to potential toxicity at specific target site. From the recent findings it was observed that biosynthesized CuNPs has potential cytotoxic efficiency against both A549 and MCF-7 cell lines. Numerous studies have reported the cytotoxic effect of plant mediated CuNPs against different cell lines. However, the exact signalling mechanism underlying cytotoxicity is still evolving. Based on the present findings and observations a probable schematic mechanistic input has been represented to understand the cause and effect of CuNPs induced cytotoxicity (Fig. 12).

According to different literature survey, generation of reactive oxygen species (ROS) has been considered as one of the major cause of toxicity *in vitro* induced by phyto-mediated nanoparticles. The mechanism

of action mainly lies with either direct interaction of CuNPs with the surface of the cancer cells after exposure or by dissolution of metal ions thus, inducing oxidative stress. Therefore, in order to reduce the toxic impact of metal ions released from NPs the capping of NPs is done with biological reducers which showed greater stability and cytotoxicity towards cancer cells *in vitro* [49]. Thus, the green method of synthesizing CuNPs could be considered safe for its use as cancer therapeutics.

It has been reported that cells undergo trillions of oxidative hits per day. Controlled generation of ROS helps to maintain controlled cellular proliferation and differentiation. But for some reason if the ROS levels increase (due to aerobic glycolysis) or scavenged ROS decrease, then the cells undergo a certain condition called oxidative stress [50]. Excessive intracellular ROS production may cause DNA damage (attributed to DNA fragmentation), cell cycle arrest, apoptosis, cytotoxicity, genotoxicity and alterations in cellular motility. In addition, ROS oxidises DNA and RNA's complementary bases, which results in genetic mutations and organism damage [51]. However, alterations in DNA leads to overexpression of tumor suppressor genes i.e., p53 and p21 which in turn induces apoptosis and inhibits cell cycle [52]. Synthesis of CuO NPs using *E. globulus* leaf extract and *Beta vulgaris* extract inhibits cell cycle at G2/M phase in MCF-7 and A549 cancer cells, respectively [53]. The ROS induced toxicity depends on shape, size and chemical composition of CuNPs. Small sized NPs have large surface to volume ratio which leads to greater ROS formation inducing cytotoxicity [27].

ROS induced programmed cell death is initiated by cysteine dependent proteases called caspases. Apoptosis involves intrinsic and extrinsic pathways which lead to formation of apoptotic bodies that are finally removed by neighbouring phagocytes [54]. The intrinsic pathway implies activation of proapoptotic proteins Bak/Bax expression on mitochondrial membrane followed by Bcl-2 induced membrane permeabilization and liberation of cytochrome c into the cytoplasm. This cyt-c combines with procaspase-9 and Apaf-1 adaptor to form apoptosome which further instigates caspase cascade pathway causing apoptosis [55]. Extrinsic pathway involves interaction of death ligand-receptor on the cell surface for activation of caspase-8. Further activation of executioner caspases 3, 7 leads to cleavage of proteins and cytoskeleton causing cell death. Dey et al. [56] reported the upregulation of intrinsic and extrinsic protein such as Bax, cyt-c, caspase 7/9 and caspase 8 in CuONPs treated MCF-7 and HeLa cell lines implying efficiency to initiate apoptosis.

Taking to the fact, CuNPs exert toxicity on cancer cell lines through various signalling methods including ROS generation, programmed cell death, antioxidant activity, cell cycle arrest, etc. The mode of action of plant extract synthesized CuNPs mainly depend upon the potential route of uptake, source and translocation pathways of Cu NPs and the type of cell line used for study. Therefore, it’s important to understand the molecular mechanism as well as its effects in order to provide better input in the field of biomedicine.

4 Conclusion

Dillenia indica is an underutilized plant valued for its medicinal uses and constitutes bioactive phytochemicals. The present study reported for the first time to synthesize CuNPs using ethanolic bark extract of *Dillenia indica* as bio-reductant. Such synthesized CuNPs were spherical in shape with a size ranging from 5–30 nm, well dispersed and possessed a highly negative zeta potential value − 41.8 mV with a stability up to one month as observed. It appears that the phytoconstituents of *D. indica* bark extract were responsible for bio-reduction process during the synthesis of CuNPs and also act as capping agents to stabilize the CuNPs. Moreover, the cytotoxicity of CuNPs, $CuCl_2$ and extract was compared and analyzed through MTT assay in dose and concentration dependent manner in A549 and MCF-7 cancer cells. Nuclear fluorescent staining by AO/EtBr and DAPI dyes indicates CuNPs induced apoptotic related cytomorphological alterations in both the cell lines. Further investigation is warranted to establish the efficiency and biocompatibility of such synthesized CuNPs with *in vivo* study to ascertain these as anticancer agents.

Declarations

Acknowledgment

The authors acknowledge the Director, CSIR-IMMT, Bhubaneswar, Odisha for his constant support and encouragement. The authors are further thankful to Imgenex, Bhubaneswar, India for providing cell lines to conduct the experiment. Ms. Larica Mohanta also gratefully thanks CSIR-HRDG, Govt. of India, New Delhi for awarding CSIR-NET Junior Research Fellowship.

Funding Information

This research work was supported by grant received from Council of Scientific and Industrial Research (CSIR-HRDG), New Delhi, Govt. of India as Research Fellowship to Ms. Larica Mohanta (File No: 31/009(0151)/2019-EMR-I).

Author contributions

1. Bhabani Sankar Jena (corresponding author)

Contribution: conceptualization, experimental design, supervision, validation, review and editing.

2. Larica Mohanta (first author)

Contribution: methodology, experiments, investigation, data analysis and interpretation, preparation of the manuscript.

Data availability

All data generated or analyzed during this study have been included in the manuscript.

Compliance with ethical standards

Ethical approval

This article does not contain any studies with human participants or animals performed by any of the authors.

Competing Interests

The authors declare no competing interests.

References

1. Y. Tauran, A. Brioude, A.W. Coleman, M. Rhimi, B. Kim, World J. Biol. Chem. **4**, 35 (2013)
2. K.B. Narayanan, N. Sakthivel, Adv. Colloid Interface Sci. **156**, 1 (2010)
3. R.R. Remya, S.R.R. Rajasree, L. Aranganathan, T.Y. Suman, Biotechnol. Rep. **8**, 110 (2015)
4. V.V. Makarov, A.J. Love, O.V. Sinitsyna, S.S. Makarova, I.V. Yaminsky, M.E. Taliansky, N.O. Kalinina, “Green” Nanotechnologies: Synthesis of Metal Nanoparticles Using Plants (2014)
5. M. Noruzi, Bioprocess. Biosyst Eng. **38**, 1 (2015)
6. D. Mott, J. Galkowski, L. Wang, J. Luo, C.J. Zhong, Langmuir **23**, 5740 (2007)
7. B. Shi, Y. Yuan, M. Jin, M.B. Betancor, D.R. Tocher, L. Jiao, D. Song, Q. Zhou, Aquaculture 532, (2021)
8. S. Adewale Akintelu, A. Kolawole Oyebamiji, S.Charles Olugbeko, and D. Felix Latona, Current Research in Green and Sustainable Chemistry **4**, (2021)
9. B.K. Park, S. Jeong, D. Kim, J. Moon, S. Lim, J.S. Kim, J. Colloid Interface Sci. **311**, 417 (2007)
10. V. Kumar, S. Kumar, V. Kumar, O. Prakash, *Antidiabetic and Antihyperlipidemic Effects of Dillenia Indica (L.) Leaves Extract* (2011)
11. N. Deepa, B.S. Jena, Int. J. Food Prop. **14**, 1152 (2011)
12. M.N. Parvin, M.S. Rahman, M.S. Islam, M.A. Rashid, Bangladesh J. Pharmacol. **4**, 122 (2009)
13. A.S. Mohanty, B.S. Jena, J. Colloid Interface Sci. **496**, 513 (2017)
14. M.I. Alahmdi, S. Khasim, S. Vanaraj, C. Panneerselvam, M.A.A. Mahmoud, S. Mukhtar, M.A. Alsharif, N.S. Zidan, N.E. Abo-Dya, O.F. Aldosari, J. Inorg. Organomet. Polym. Mater. **32**, 2146 (2022)
15. L.A. Torre, R.L. Siegel, A. Jemal, Adv. Exp. Med. Biol. **893**, 1 (2016)
16. J. Ferlay, I. Soerjomataram, R. Dikshit, S. Eser, C. Mathers, M. Rebelo, D.M. Parkin, D. Forman, F. Bray, Int. J. Cancer **136**, E359 (2015)
17. M. Thun, R. Peto, J. Boreham, A.D. Lopez, Tob. Control **21**, 96 (2012)
18. N. Parsa, *Environmental Factors Inducing Human Cancers* (2012)
19. D. Singh, V. Kumar, E. Yadav, N. Falls, M. Singh, U. Komal, A. Verma, IET Nanobiotechnol. **12**, 748 (2018)
20. T. Akther, V. Mathipi, N.S. Kumar, M. Davoodbasha, H. Srinivasan, Environ. Sci. Pollut. Res. **26**, 13649 (2019)

21. M. Vairavel, E. Devaraj, R. Shanmugam, Environ. Sci. Pollut. Res. **27**, 8166 (2020)
22. U.R. Shwetha, M.S. Latha, C.R. Rajith Kumar, M.S. Kiran, V.S. Betageri, J. Inorg. Organomet. Polym. Mater. **30**, 4876 (2020)
23. M. Valodkar, R.N. Jadeja, M.C. Thounaojam, R.V. Devkar, S. Thakore, Mater. Chem. Phys. **128**, 83 (2011)
24. I. Chung, A.A. Rahuman, S. Marimuthu, A.V. Kirthi, K. Anbarasan, P. Padmini, G. Rajakumar, Exp. Ther. Med. **14**, 18 (2017)
25. E.E. Elemike, D.C. Onwudiwe, M. Singh, J. Inorg. Organomet. Polym. Mater. **30**, 400 (2020)
26. D.B. Manikandan, M. Arumugam, S. Veeran, A. Sridhar, R. Krishnasamy Sekar, B. Perumalsamy, T. Ramasamy, Environ. Sci. Pollut. Res. **28**, 33927 (2021)
27. M. Hasanin, M.A. al Abboud, M.M. Alawlaqi, T.M. Abdelghany, A.H. Hashem, Biol. Trace Elem. Res. **200**, 2099 (2022)
28. D. Rehana, D. Mahendiran, R.S. Kumar, A.K. Rahiman, Biomed. Pharmacotherapy **89**, 1067 (2017)
29. N. Senthilkumar, E. Nandhakumar, P. Priya, D. Soni, M. Vimalan, and I. Vetha Potheher, New Journal of Chemistry **41**, 10347 (2017)
30. T. Dutta, A. Paul, M. Majumder, R.A. Sultan, and T. Bin Emran, Biochem Biophys Rep **21**, (2020)
31. S.B. Kntayya, M.D. Ibrahim, N.M. Ain, R. Iori, C. Ioannides, and A. F. Abdull Razis, Nutrients 10, (2018)
32. X. Weng, M. Guo, F. Luo, Z. Chen, Chem. Eng. J. **308**, 904 (2017)
33. M.I. Din, F. Arshad, Z. Hussain, M. Mukhtar, Nanoscale Res Lett 12, (2017)
34. N. Nagar, V. Devra, Mater. Chem. Phys. **213**, 44 (2018)
35. S.C.G. Kiruba Daniel, G. Vinothini, N. Subramanian, K. Nehru, M. Sivakumar, Journal of Nanoparticle Research 15, (2013)
36. M. Vaseem, K.M. Lee, D.Y. Kim, Y.B. Hahn, Mater. Chem. Phys. **125**, 334 (2011)
37. S. Yallappa, J. Manjanna, M.A. Sindhe, N.D. Satyanarayan, S.N. Pramod, K. Nagaraja, Spectrochim Acta A Mol Biomol Spectrosc **110**, 108 (2013)
38. S.S. Momeni, M. Nasrollahzadeh, A. Rustaiyan, J. Colloid Interface Sci. **472**, 173 (2016)
39. M. Gondwal and G. Joshi Nee Pant, Int J Biomater 2018, (2018)
40. A. Ahmed, M. Usman, Q.Y. Liu, Y.Q. Shen, B. Yu, H.L. Cong, Ferroelectrics **549**, 61 (2019)
41. R. Sankar, R. Maheswari, S. Karthik, K.S. Shivashangari, V. Ravikumar, Mater. Sci. Eng., C **44**, 234 (2014)
42. S. Harne, A. Sharma, M. Dhaygude, S. Joglekar, K. Kodam, M. Hudlikar, Colloids Surf. B Biointerfaces **95**, 284 (2012)
43. M.A. Siddiqui, R. Wahab, J. Ahmad, N.N. Farshori, A.A. Al-Khedhairy, J. Inorg. Organomet. Polym. Mater. **30**, 4106 (2020)
44. F. Liu, S. Gao, Y. Yang, X. Zhao, Y. Fan, W. Ma, D. Yang, A. Yang, Y. Yu, Oncol. Lett. **14**, 2775 (2017)
45. D. Solairaj, P. Rameshthangam, G. Arunachalam, Int. J. Biol. Macromol. **105**, 608 (2017)

46. B.-Y. Choi, H.-Y. Kim, K.-H. Lee, Y.-H. Cho, G. Kong, S. Korea, *Clo®lium, a Potassium Channel Blocker, Induces Apoptosis of Human Promyelocytic Leukemia (HL-60) Cells via Bcl-2-Insensitive Activation of Caspase-3* (n.d.)
47. S. Sreelatha, A. Jeyachitra, P.R. Padma, Food Chem. Toxicol. **49**, 1270 (2011)
48. J. Baharara, F. Namvar, T. Ramezani, M. Mousavi, R. Mohamad, Molecules **20**, 2693 (2015)
49. F. Perreault, R. Popovic, D. Dewez, Environ. Pollut. **185**, 219 (2014)
50. B. Perillo, M. Di Donato, A. Pezone, E. Di Zazzo, P. Giovannelli, G. Galasso, G. Castoria, A. Migliaccio, Exp. Mol. Med. **52**, 192 (2020)
51. J.T. Buchman, N.V. Hudson-Smith, K.M. Landy, C.L. Haynes, Acc. Chem. Res. **52**, 1632 (2019)
52. D. Letchumanan, S.P.M. Sok, S. Ibrahim, N.H. Nagoor, N.M. Arshad, Biomolecules 11, (2021)
53. R. Chandrasekaran, S.A. Yadav, S. Sivaperumal, J. Clust Sci. **31**, 221 (2020)
54. J. Chandra, A. Samali, S. Orrenius, Free Radic Biol Med **29**, 323 (2000)
55. C.M. Pfeffer, A.T.K. Singh, Int J Mol Sci 19, (2018)
56. A. Dey, S. Manna, S. Chattopadhyay, D. Mondal, D. Chattopadhyay, A. Raj, S. Das, B.G. Bag, S. Roy, J. Saudi Chem. Soc. **23**, 222 (2019)

Figures

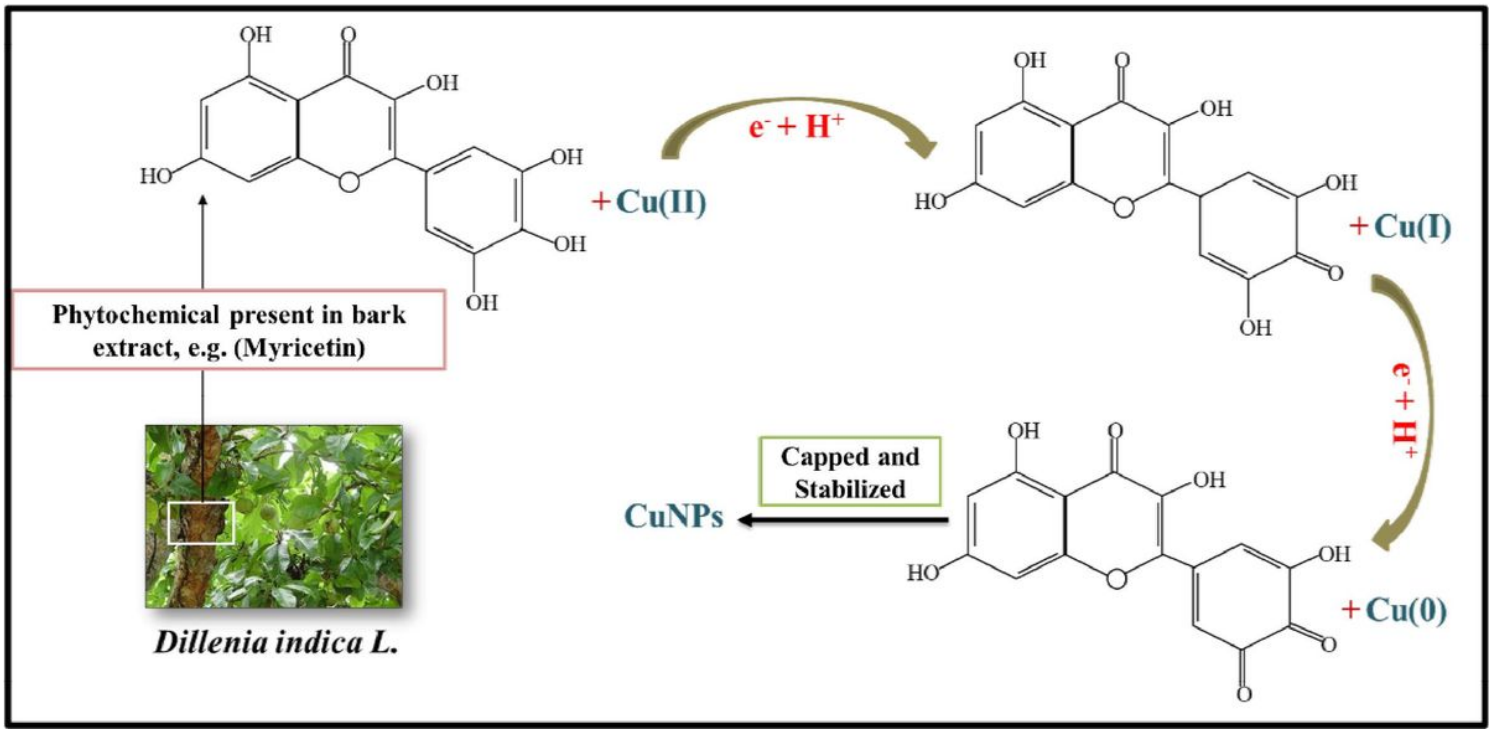

Figure 1

Plausible reduction mechanism of copper metal into CuNPs by *Dillenia indica* bark extract

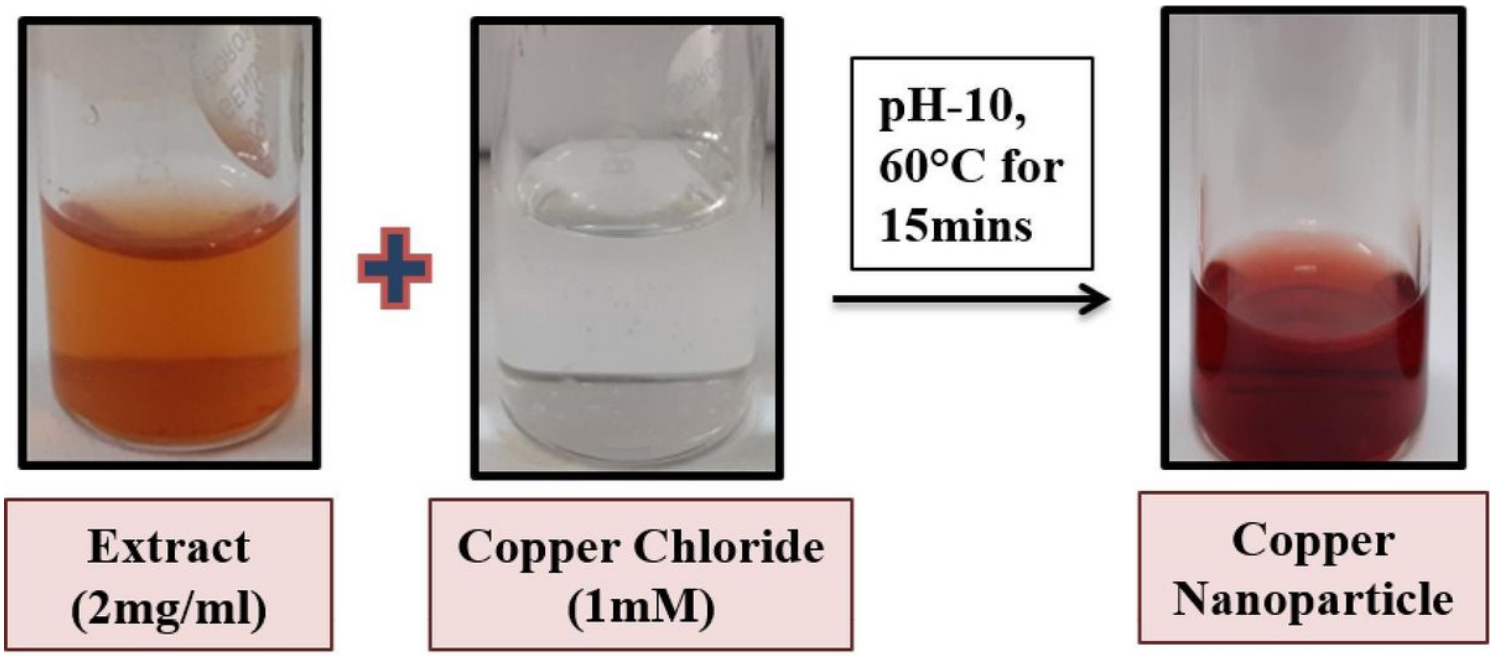

Figure 2

Synthesis of CuNPs using ethanolic bark extract of *Dillenia indica*

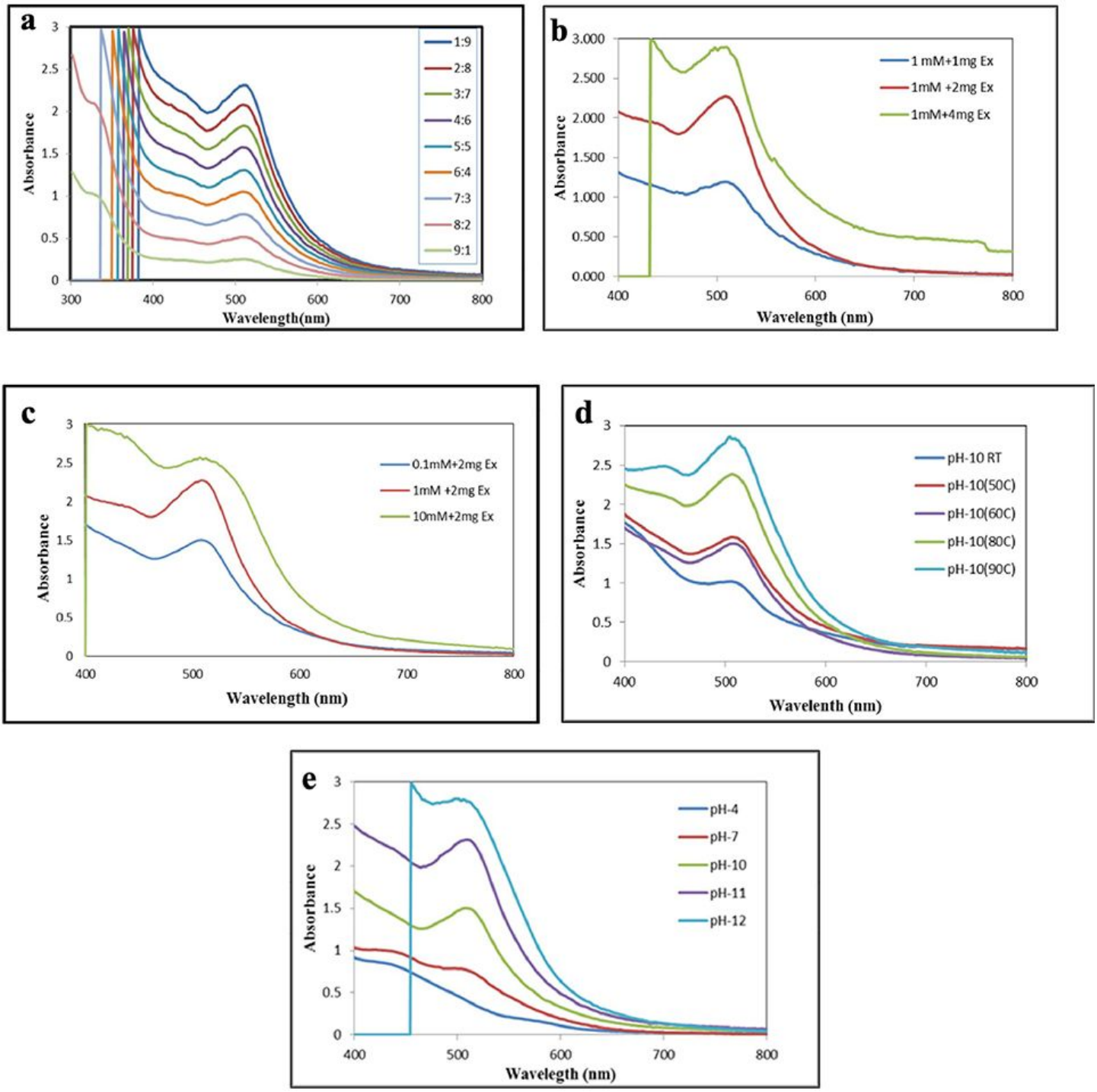

Figure 3

Optimization of CuNPs synthesis parameters: (a) Mixing ratio of extract & $CuCl_2$, (b) Concentration of bark extract, (c) Molarity of Copper Chloride, (d) Effect of pH, (e) Effect of Temperature

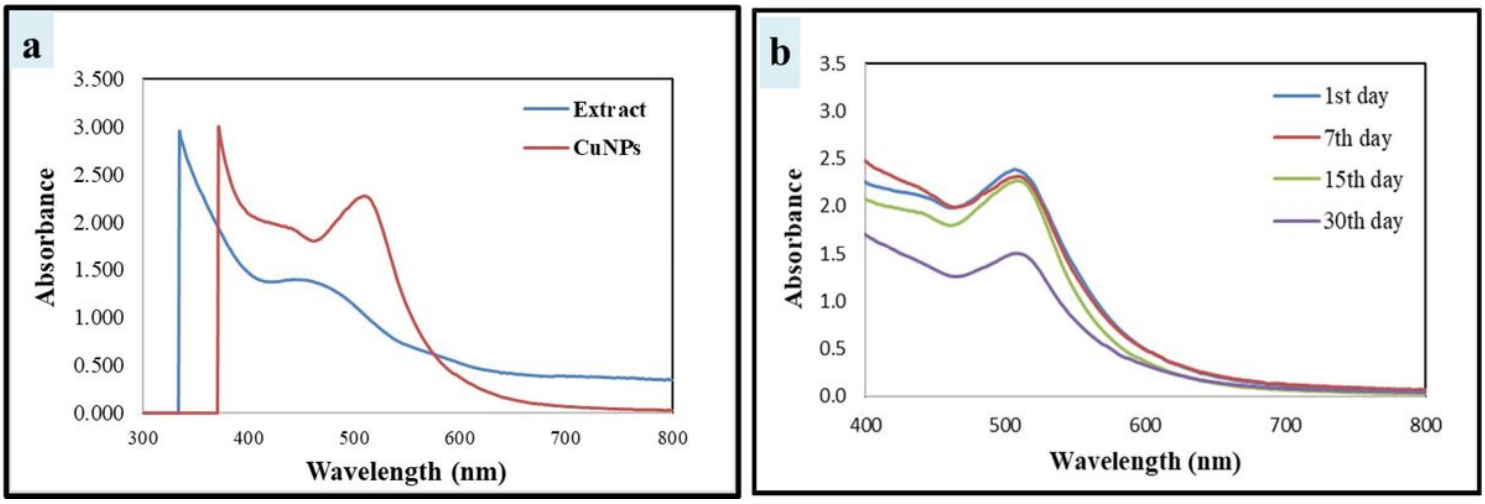

Figure 4

UV- visible absorption spectra of (a) biosynthesized CuNPs & *D. indica* bark extract and (b) CuNPs between 1st day to 30th day

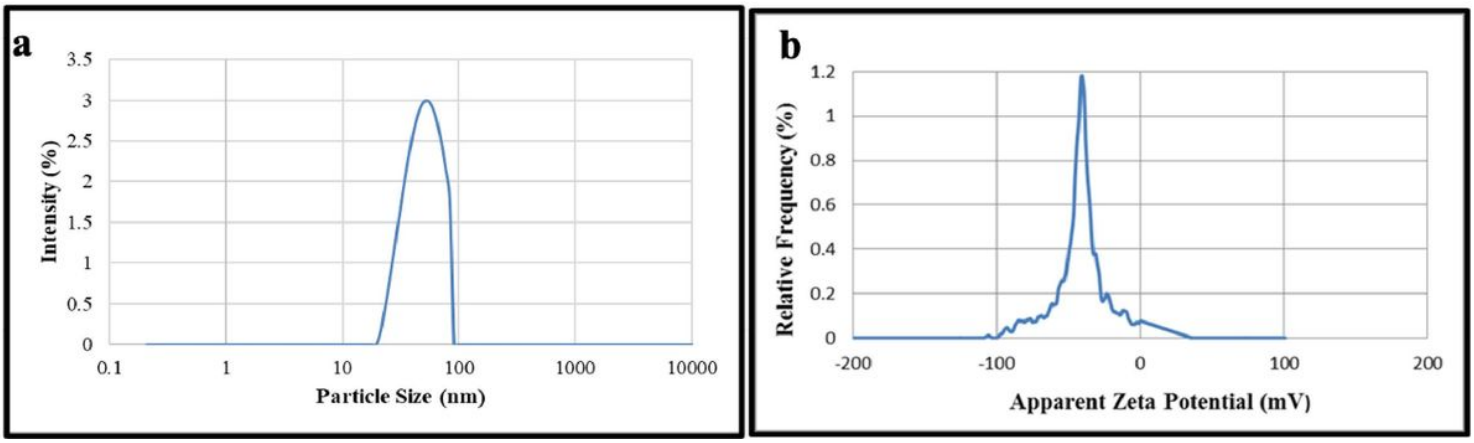

Figure 5

(a) Particle size distribution and (b) Zeta Potential analysis

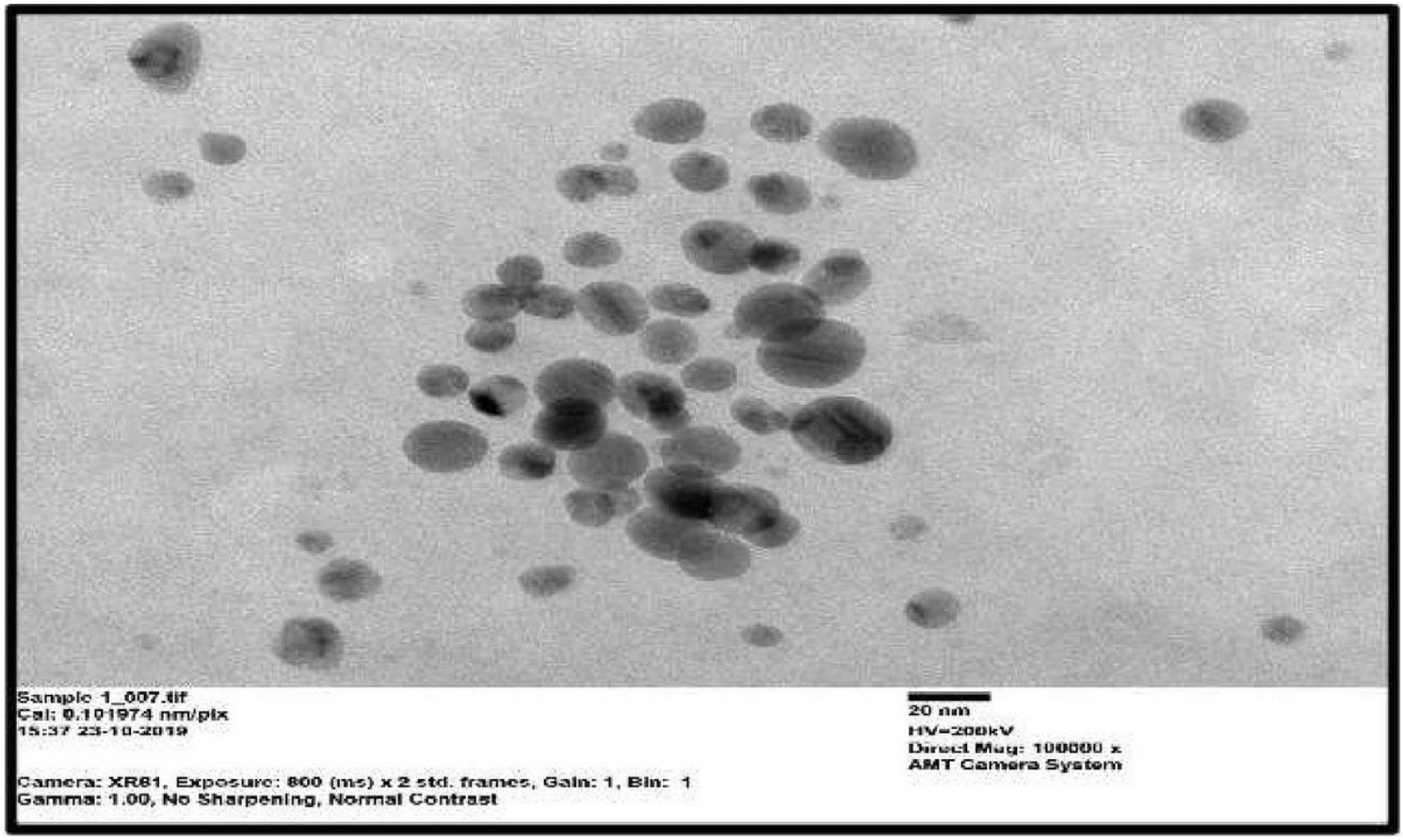

Figure 6

TEM images of synthesized CuNPs at 20 nm scale

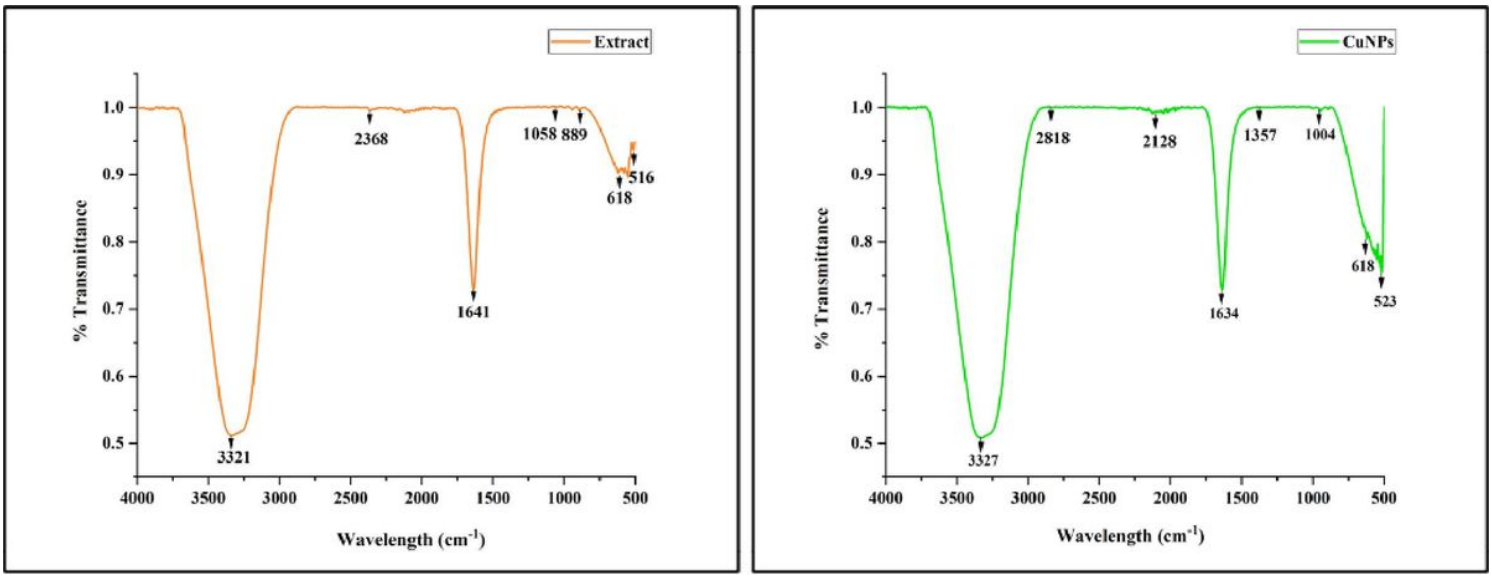

Figure 7

FTIR spectra of synthesized CuNPs and *D. indica* bark extract

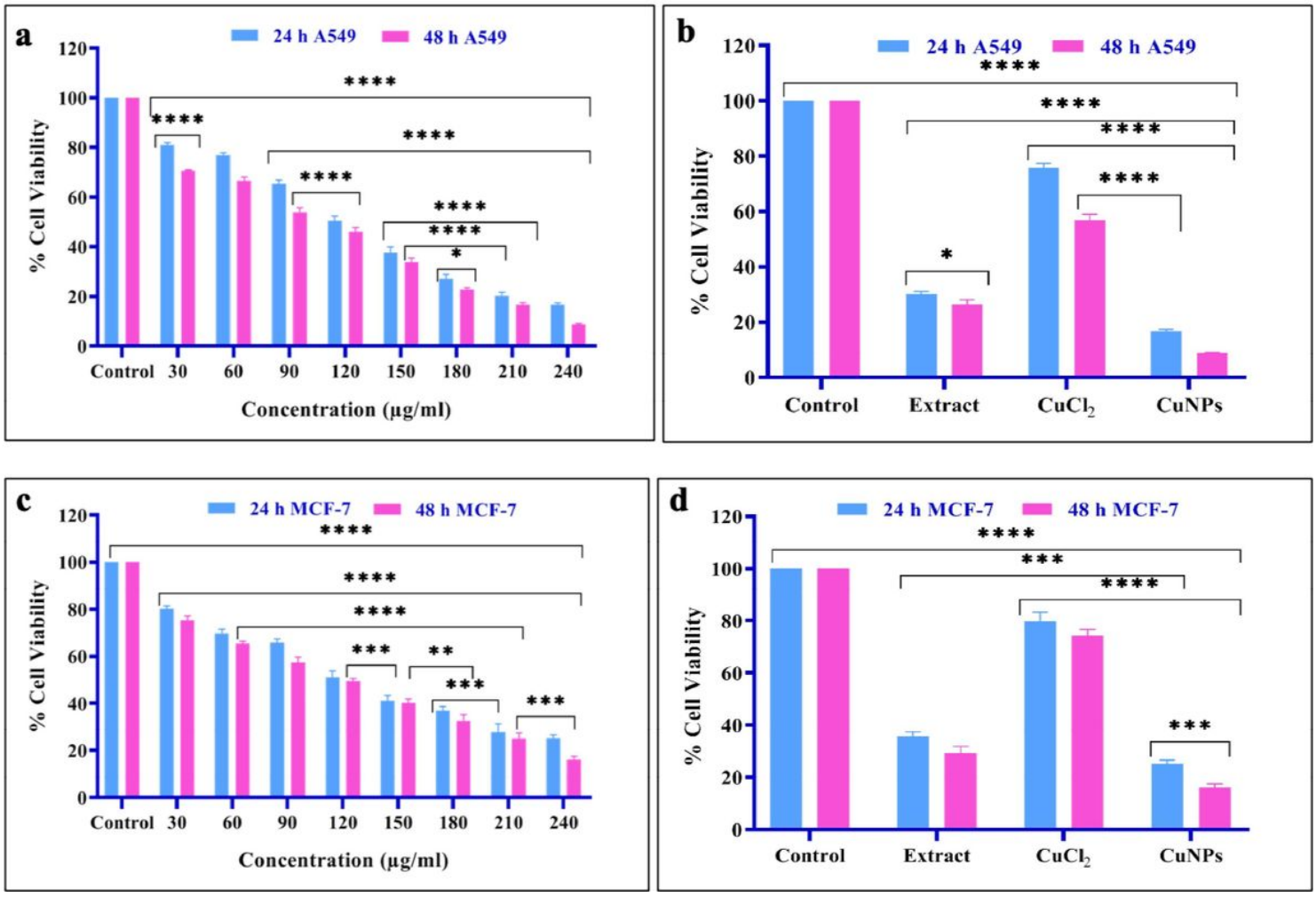

Figure 8

Significant concentration and time dependent cell viability studies of (a) CuNPs treated A549 cells, (b & d) comparison of cytotoxicity between control, extract, $CuCl_2$ and CuNPs (c) CuNPs treated MCF-7 cells after 24 h and 48 h. Data expressed as mean ± SEM of the absorbance. * $p<0.05$, ** $p<0.01$, ***$p<0.001$ & * $p<0.0001$ indicated the significance differences (ANOVA followed by Tukey's Test, $\alpha<0.05$)

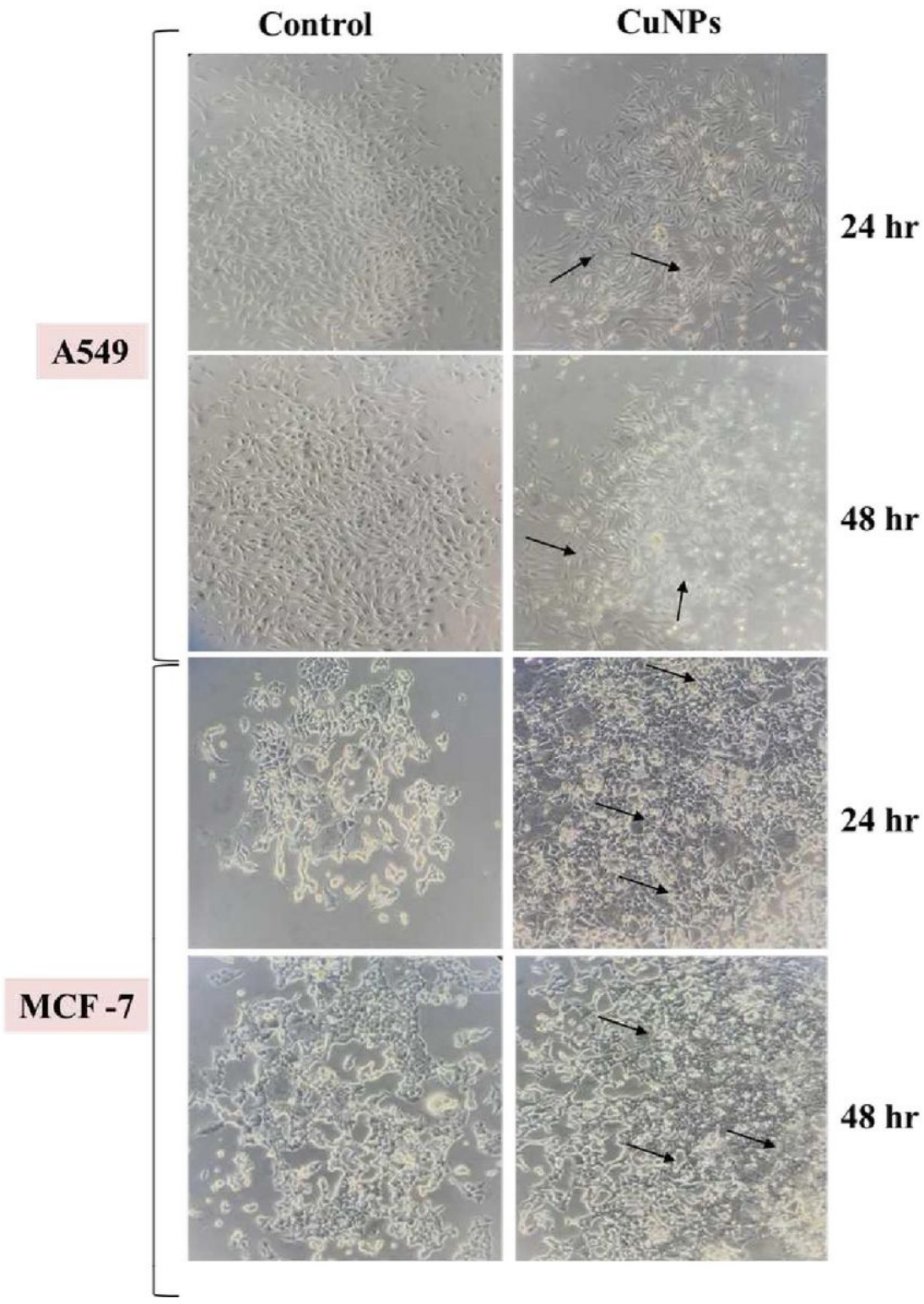

Figure 9

Representative morphological changes of Control (without treatment) and CuNPs treated A549 and MCF-7 cells for 24 h and 48 h. Arrows specify cellular shrinkage, clumped shapes and apoptotic bodies in treated cells.

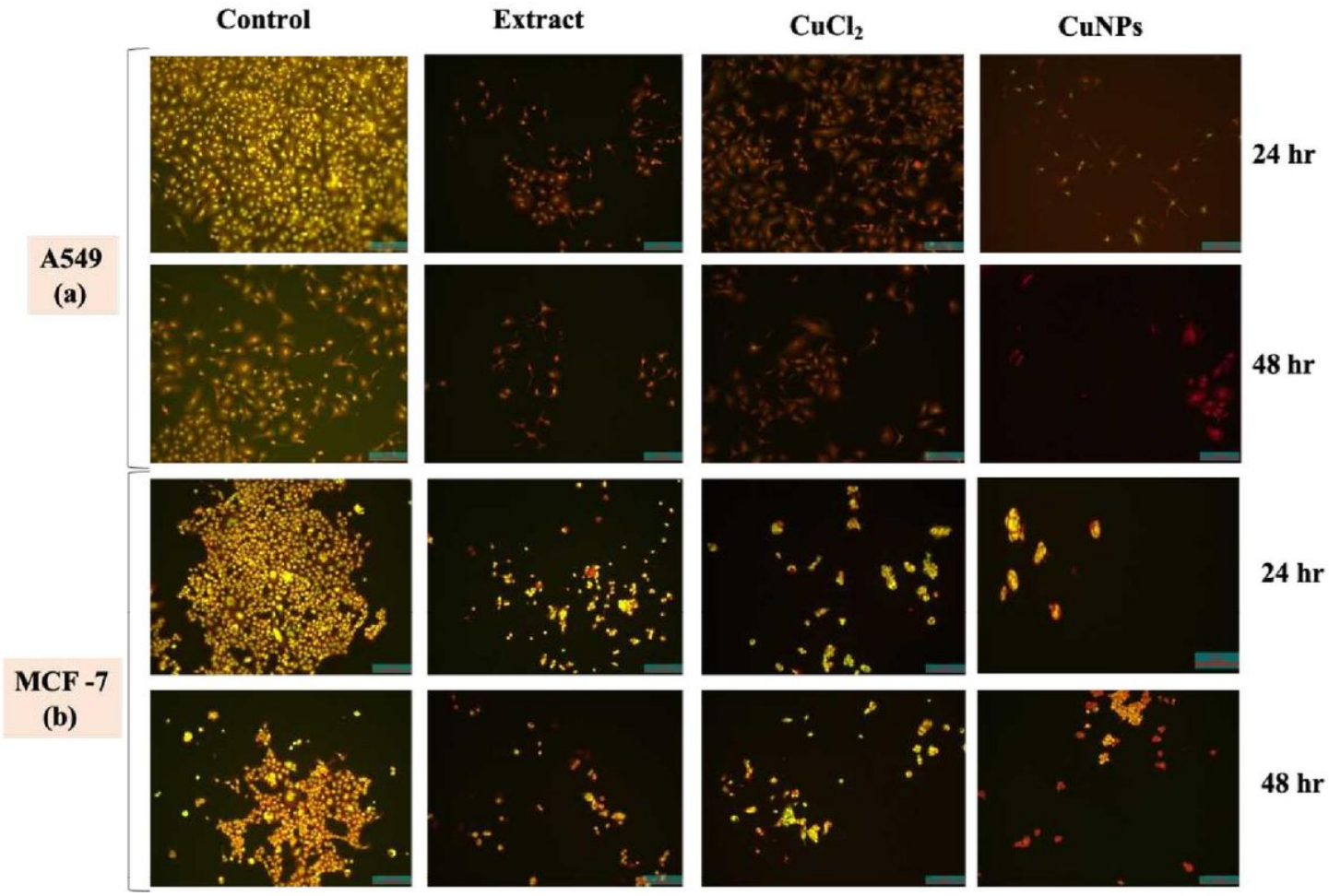

Figure 10

AO/EtBr staining of (a) A549 after 24 & 48 hr and (b) MCF-7 after 24 & 48 hr. Images were taken in fluorescence microscope at 10X magnification.

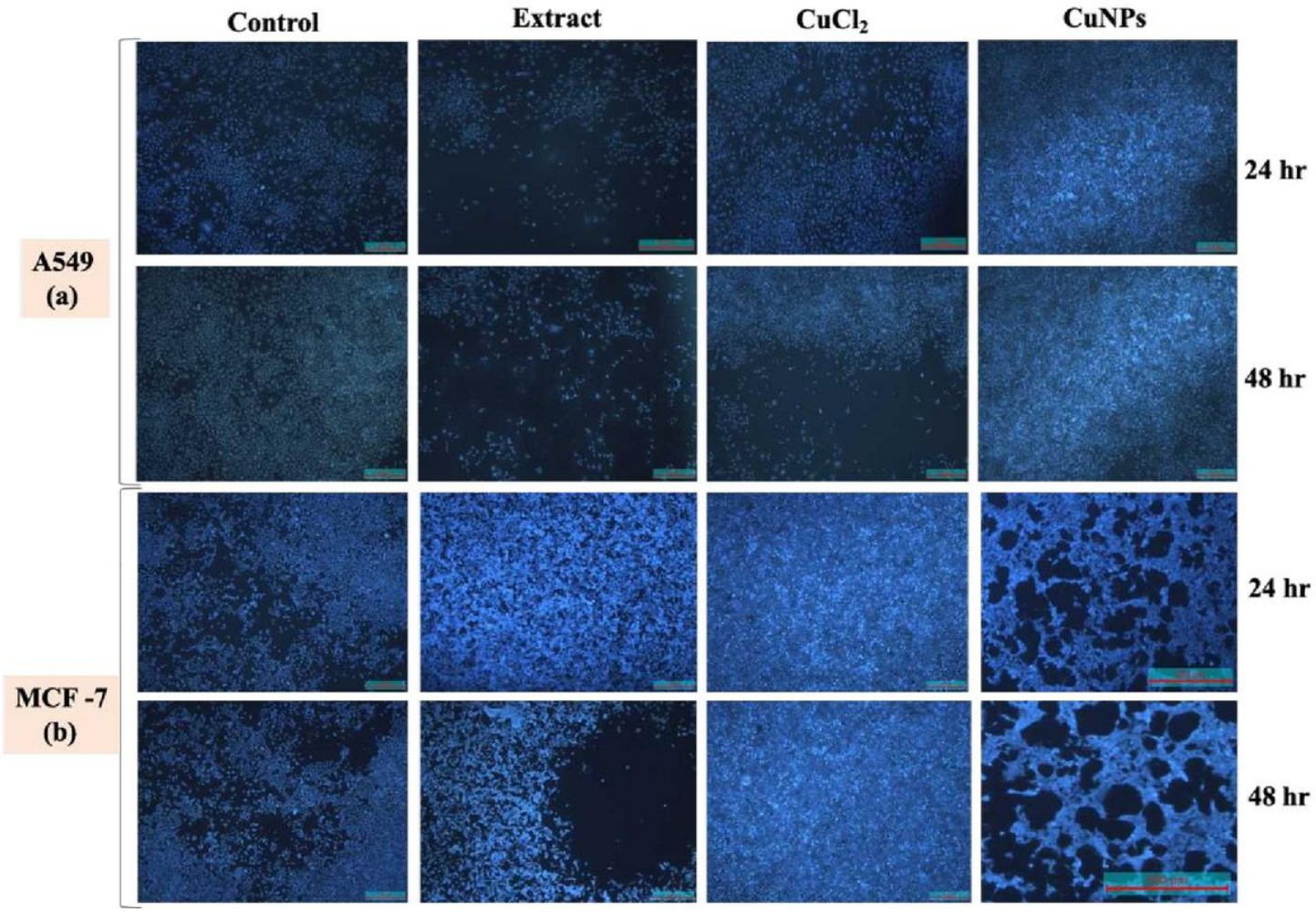

Figure 11

DAPI staining of (a) A549 after 24 & 48 hr and (b) MCF-7 after 24 & 48 hr

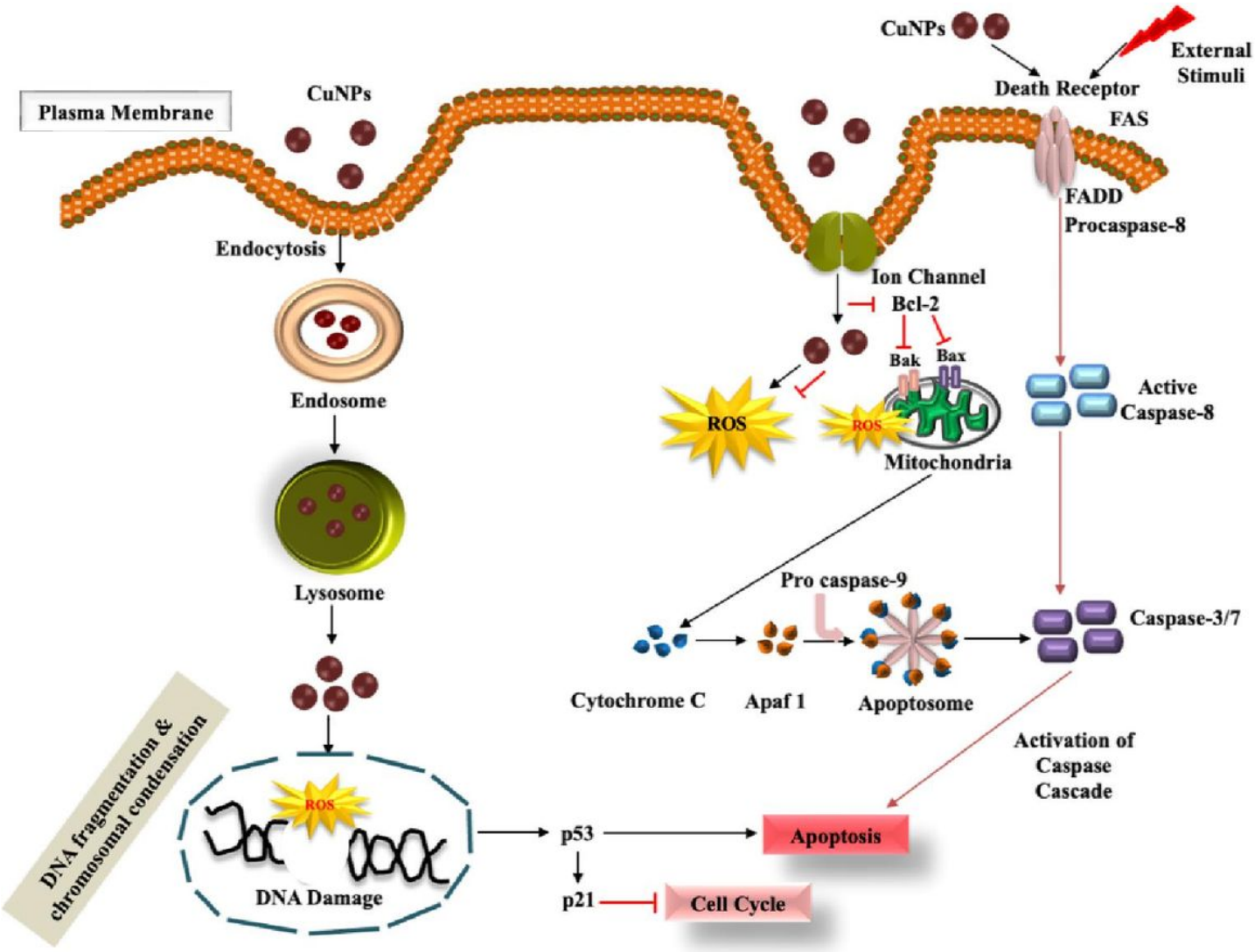

Figure 12

Schematic illustration of the cytotoxic potency of plant mediated CuNPs